Perception & Psychophysics
1999, 61 (6), 1075-1088

Second-order reversed phi

ZHONG-LIN LU
University of Southern California, Los Angeles, California

and

GEORGE SPERLING
University of California, Irvine, California

In a first-order reversed-phi motion stimulus (Anstis, 1970), the black–white contrast of successive frames is reversed, and the direction of apparent motion may, under some conditions, appear to be reversed. It is demonstrated here that, for many classes of stimuli, this reversal is a mathematical property of the stimuli themselves, and the real problem is in perceiving forward motion, which involves the second- or third-order motion systems or both. Three classes of novel second-order reversed-phi stimuli (contrast, spatial frequency, and flicker modulation) that are invisible to first-order motion analysis were constructed. In these stimuli, the salient stimulus features move in the *forward* (feature displacement) direction, but the second-order motion energy model predicts motion in the *reversed* direction. In peripheral vision, for all stimulus types and all temporal frequencies, all the observers saw only the reversed-phi direction of motion. In central vision, the observers also perceived reversed motion at temporal frequencies above about 4 Hz, but they perceived movement in the forward direction at lower temporal frequencies. Since all of these stimuli are invisible to first-order motion, these results indicate that the second-order reversed-phi stimuli activate two subsequent competing motion mechanisms, both of which involve an initial stage of texture grabbing (spatiotemporal filtering, followed by fullwave rectification). The second-order motion system then applies a Reichardt detector (or equivalently, motion energy analysis) directly to this signal and arrives at the reversed-phi direction. The third-order system marks the location of features that differ from the background (the figure) in a salience map and computes motion in the forward direction from the changes in the spatiotemporal location of these marks. The second-order system's report of reversed movement dominates in peripheral vision and in central vision at higher temporal frequencies, because it has better spatial and temporal resolution than the third-order system, which has a cutoff frequency of 3–4 Hz (Lu & Sperling, 1995b). In central vision, below 3–4 Hz, the third-order system's report of resolvable forward movement of something salient (the figure) dominates the second-order system's report of texture contrast movement.

There is mounting evidence that there are three parallel streams of visual motion computation—first- and second-order systems that are primarily monocular and a third-order binocular system (Lu & Sperling, 1995a, 1995b, 1996c). The first-order system extracts motion from drifting luminance modulations, and the second-order system extracts motion from drifting texture contrast modulations. These primarily monocular systems use motion energy analyses (Adelson & Bergen, 1985) or, equivalently, elaborated Reichardt detectors (van Santen & Sperling, 1984, 1985). Both primarily monocular systems are fast (temporal cutoff frequency at 10–12 Hz) and approximately equally sensitive to a wide range of spatial frequencies (0.6–4.8 cpd). These relations are illustrated in Figure 1. The third-order system is binocular, in the sense that it is indifferent to the eye or eyes of origin of successive images. When successive images alternate between eyes, so that motion extraction requires the combination of left-eye and right-eye information, only the third-order system is effective.

Lu and Sperling (1995a) proposed that the third-order system derives its input from a dynamic salience map that records the moment-to-moment positions of the most salient stimulus features (i.e., figure vs. ground). The motion of areas marked as *figure* is computed from this dynamic map, just as the movement of areas marked by more (or fewer) photons is computed by the first-order motion system and the movement of areas marked by more (or fewer) features is computed by the second-order system. The third-order motion system is relatively slower (temporal cutoff frequency is 3–4 Hz), has lower spatial resolution than the first- or second-order system (Lu & Sperling, 1995b), and can be influenced by attentional instructions (Lu & Sperling, 1995a).

Nishida (1993) first observed second-order reversed phi. Here, we describe novel demonstrations of second-

This research was supported by AFOSR, Life Science Directorate, Visual Information Processing Program. Correspondence concerning this article should be addressed to Z.-L. Lu, Department of Psychology, SGM501, University of Southern California, Los Angeles, CA 90089 (e-mail: zhonglin@ref.usc.edu), or G. Sperling, Department of Cognitive Sciences, SSPA-3, University of California, Irvine, CA 92697 (e-mail: sperling@uci.edu).

—Accepted by previous editor, Myron L. Braunstein

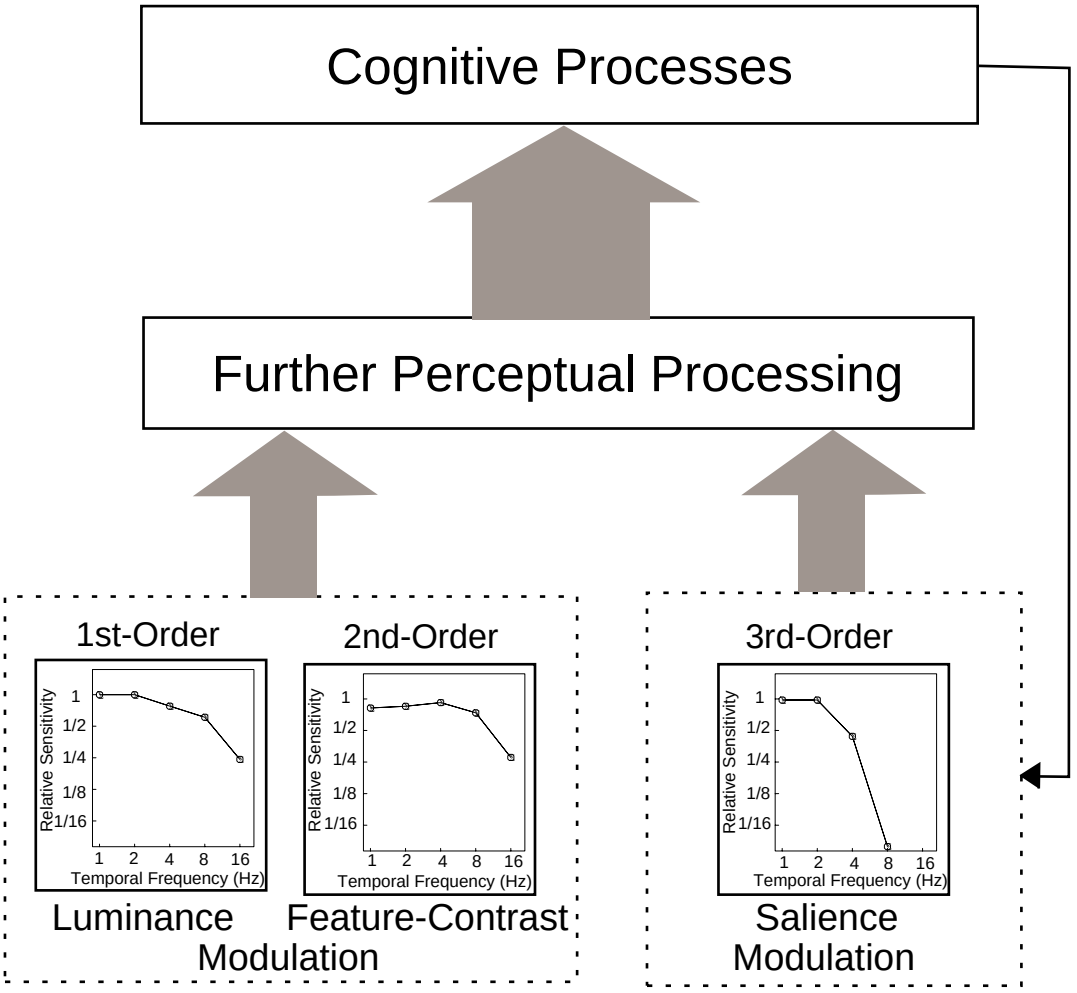

Figure 1. Functional organization of human visual motion perception (after Lu & Sperling, 1995b). Two parallel streams of motion computation are shown: first-order (luminance) and second-order (contrast) modulation systems on the left side, and the third-order (salience) motion computation on the right side. In first-order motion, motion energy is computed directly from raw stimulus point contrast; the second-order system computes motion energy from spatiotemporally filtered and rectified stimulus contrast (contrast variance). The graphs of relative sensitivity versus temporal frequency (from Lu & Sperling, 1995b) show that both first- and second-order motion systems are equally fast (temporal frequency cutoff ≈ 12 Hz); they are primarily monocular, bottom-up, and sensitive to a wide range of spatial frequencies. Third-order motion is inherently binocular, slower (temporal frequency cutoff ≈3 Hz), and has coarser spatial resolution. Unlike first- and second-order motion, the third-order motion computation is partially top-down controlled—it can be strongly influenced by attention.

order reversed phi that yield a different kind of evidence supporting (1) the existence of independent second- and third-order motion computations plus (2) the hypothesis that second-order motion computation, like first-order computation, is a motion energy computation (Chubb & Sperling, 1988, 1991). That is, motion is extracted from second-order stimuli by motion energy analysis of the stimuli after spatiotemporal bandpass filtering and full-wave rectification. We first present a mathematical analysis of a simple class of very effective reversed-phi stimuli to illustrate why reversed-phi stimuli reverse apparent direction, and we briefly review the analysis of motion perception systems, because these are critical to understanding the second-order experiments.

Motion Energy Analysis (Standard Motion Analysis, Elaborated Reichardt Model)

To extract texture orientation, Knutsson and Granlund (1983) used a spatial sinewave and a cosinewave filter with the to-be-extracted orientation, squared the outputs of these filters, and added them. This quadrature operation extracts the total stimulus energy at that orientation, independent of the spatial phase of the stimulus. Figure 2a shows two examples of the computation of orientation

energy: The left side illustrates energy computed at +45°; the right side, +135°. (For an orientation energy computation, the symbol *t* in Figure 2a and subsequent figures should be read as *y*.) Watson, Ahumada, and Farrell (1986) showed that the extraction of motion direction in space–time *x*,*t* is formally equivalent to the extraction of spatial orientation in *x*,*y*. Changing the coordinates of Granlund and Knutsson's quadrature operation from *x*,*y* to space–time *x*,*t* yields a motion energy computation that gives the total motion energy in a particular direction. To decide in which one of two opposite motion directions a stimulus is moving, an optimum statistical procedure is to take the difference of the two oppositely oriented quadrature filter pairs in *x*,*t*, analogous to Granlund and Knutsson's difference in *x*,*y*. This is the motion energy model of Adelson and Bergen (1985) for judging the motion direction of drifting luminance modulations (Figure 2). Van Santen and Sperling (1985) proved that, at the system level, the motion energy model was equivalent to such earlier motion theories as (1) the elaborated Reichardt model of Figure 2b (van Santen & Sperling, 1984) and (2) the elaborated Watson–Ahumada (1983) motion filter. At a system level, all three of these models are equivalent, and Chubb and Sperling (1989b) proposed the term *standard motion analysis* for this computation. However, here we use the terms *motion energy analysis* or *motion energy computation* to refer to this computation.[1]

Second-Order Motion: Stimuli and Model

A stimulus $S(x,y,t)$ is called *drift-balanced* if the expected outputs of oppositely directed motion energy detectors are equal, no matter what their spatial or temporal frequency characteristics may be. A drift-balanced stimulus $S(x,y,t)$ is called *microbalanced* if and only if the expected output of every motion energy detector in response to this stimulus is zero. In other words, motion energy analysis cannot extract a consistent direction of motion from any microbalanced or drift-balanced stimulus. However, Chubb and Sperling (1988, 1989a; see, also, Derrington & Badcock, 1985; Lelkens & Koenderink, 1984; Ramachandran, Rao, & Vidyasagar, 1973; Sperling, 1976; Turano & Pantle 1989; Victor & Conte, 1990) induced vivid motion perception in humans, using broad classes of microbalanced stimuli that were constructed of drifting modulations of contrast, spatial frequency, texture type, or flicker. The term *second-order motion* was introduced by Cavanagh and Mather (1989) and Chubb and Sperling (1989b) to replace the earlier term *non-Fourier* motion (Chubb & Sperling, 1988) for describing classes of motion that are not directly accessible to motion energy analysis. That is, although motion energy computations successfully predict human performance in judging motion direction of drifting first-order (luminance) modulations (van Santen & Sperling, 1984), motion energy computations are essentially blind to properly constructed second-order stimuli. Motion energy computations extract no consistent motion from second-order stimuli, even though human observers see them as vividly moving (Chubb & Sperling, 1988, 1991; Zhou & Baker, 1993).

A second-order motion energy model was proposed by Chubb and Sperling (1988, 1991) for extracting motion from second-order motion stimuli (Figure 3). The model consists of three stages: (1) a linear spatiotemporal bandpass filter, (2) a fullwave rectification (e.g., absolute value or square-law rectifier), and (3) motion energy analysis. The Chubb–Sperling model is sufficient to extract second-order motion and is described in more detail below. Here, we offer further evidence, on the basis of reversed phi, that unexpected perceptual properties of complex stimuli are accurately predicted by the Chubb–Sperling model.

Reversed Phi

Phi. Exner (1875) began a tradition of studying apparent motion by using the two-stimulus method, a procedure that was most successfully exploited by Wertheimer (1912). In a typical experiment, a bar is flashed briefly at location *A*, and, after a short interval Δt, another bar is flashed briefly at a different location *B*. When the time interval Δt is appropriate, observers report seeing movement from location *A* to location *B*, even though the bar does not move from one place to the other. This is called the *phi* phenomenon. Historically, a great deal of the literature of psychophysics has been devoted to the study of the phi phenomenon. We now understand that it is just a special case of spatiotemporally sampled motion, with a sample size of two.

Reversed phi. Anstis (1970) reported a phenomenon that he called *reversed phi*. In a typical demonstration, a bar (white or black) is flashed on a neutral background at location *A* and is followed, after a brief interval, by another bar of *opposite* contrast polarity (black or white) at a nearby location *B*. Especially in peripheral vision, observers report perceiving motion in the *reversed* direction *B* to *A*, rather than in the direction of the displacement from *A* to *B* (Anstis, 1970; Anstis & Rogers, 1975; Chubb & Sperling, 1989b).

The mathematical explanation of the reversed motion in reversed phi.[2] Anstis (1970) explained reversed phi as brightness matching. Reichardt (1961), working with beetles (*Chlorophanus*), had already observed (but not named) reversed phi when successive flashes to adjacent facets of the compound eye had opposite contrasts. Reichardt explained the reversal in terms of an autocorrelation model that involved multiplying the contrasts of the two flashes. Van Santen and Sperling (1984), working with human observers, investigated reversed-phi motion in periodic stimuli in which the stimulus stepped 90° of its fundamental frequency in every time period. They proved that a Reichardt (or motion energy) detector would produce exactly as much output in the reversed direction for their reversed-phi stimuli as the original (nonreversed) stimulus produces in the forward direction. This principle is illustrated in Figure 4 and Table 1.

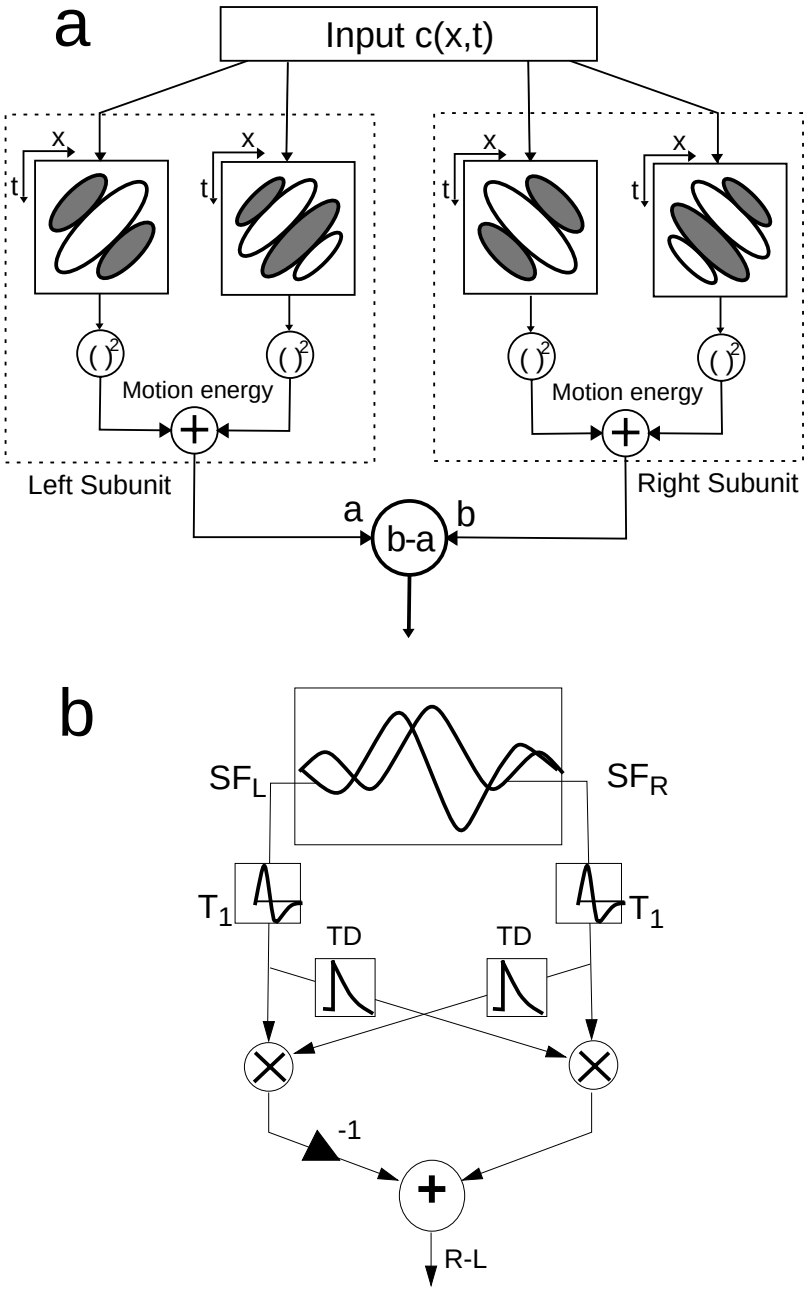

Figure 2. Panel a: A model for computing orientation energy and motion energy. For the *spatial interpretation* (Knutsson & Granlund, 1983) involving *orientation energy* (substitute the symbol *y* wherever the symbol *t* appears in the figure), the input is the point contrast $c(x,y)$ at spatial coordinates x,y. (Point contrast is luminance at a point, divided by mean luminance.) The squared outputs of a pair of similarly oriented Hubel–Wiesel line and edge detectors (cosine and sine Gabors) are added to determine orientation energy, and the two oppositely oriented energies are subtracted to determine which orientation has the most energy. All the filters are centered at the same location. The model produces a positive output for stimuli oriented at −45º and a negative output for stimuli oriented at +45º. For the *space–time interpretation* (Adelson & Bergen, 1985), involving *motion energy*, the input is point contrast $c(x,t)$ of a vertically oriented grating as a function of horizontal space x and time t. The same flowchart now describes a motion energy detector for discriminating between vertical gratings that move horizontally, either leftward or rightward. The +45º orientation energy subunit now is interpreted as a leftward movement subunit; the −45º orientation is a rightward movement subunit. Each subunit computes motion energy in its preferred direction by summing the squared outputs of a quadrature pair (e.g., cosine and sine Gabor filters), defined in space–time (x,t). Motion direction is indicated by the sign of the difference between two subunit outputs: A positive sign indicates rightward motion, a negative sign leftward motion. This overall computation is equivalent to a Reichardt model. Panel b: Reichardt model equivalent to the model shown in panel a. SF_L and SF_R indicate the left- and right-subunit spatial filters; T_1 indicates a temporal filter; TD indicates a temporal delay filter; × indicates multiplication; −1 indicates multiplication by minus one; + indicates addition; R − L indicates the output that consists of rightward minus leftward motion energy.

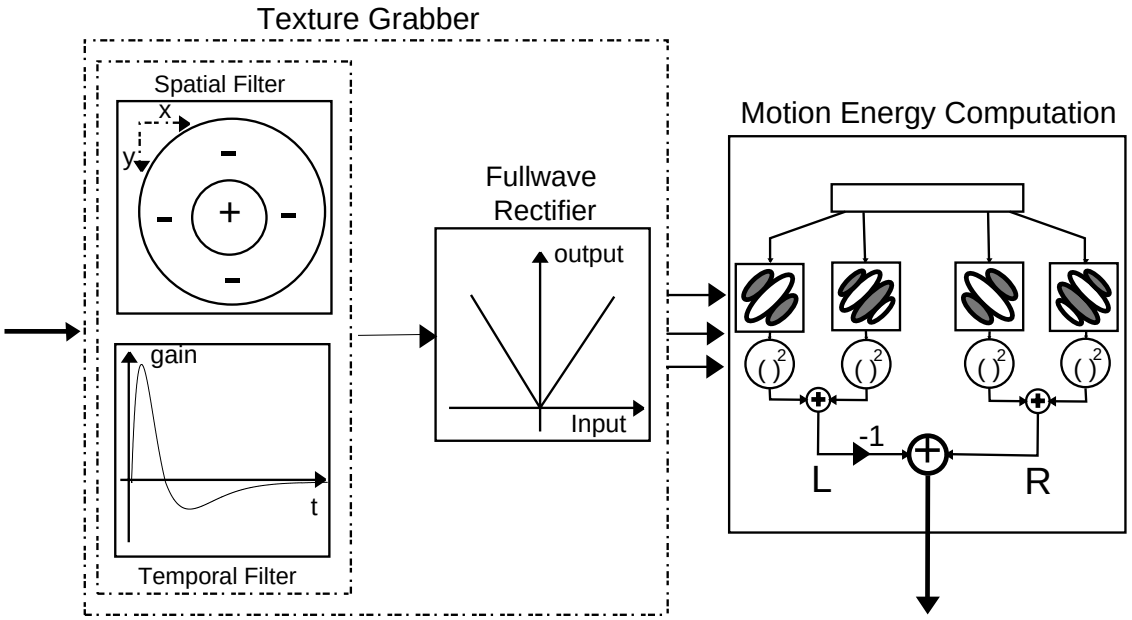

Figure 3. A second-order motion energy model. A texture grabber is followed by a motion energy detector. The texture grabber consists of a spatiotemporal linear filter. The spatial component is represented as a cosine receptive field (which is primarily sensitive to a particular orientation and spatial frequency), and the temporal component is a bandpass filter that is relatively insensitive to very low and very high temporal frequencies. Fullwave rectification (e.g., absolute value or square-law rectifier; absolute value is shown) gives the texture grabber an output that depends only on the total quantity of texture in its preferred orientation and frequency, independent of the sign of the outputs of the linear filters, which may be either positive or negative. Motion energy analysis (Figure 2) determines the direction of motion of the texture being detected by the texture grabber. This article addresses the question of whether motion energy analysis, as proposed in this flow chart, is indeed the algorithm used by second-order motion perception.

Figures 4a and 4b illustrate a normal and a reversed-phi stimulus. Figure 4c illustrates five successive frames of a sine wave, in which successive frames translate 90º to the right. Figure 4d illustrates the reversed-phi version of this stimulus, in which even frames are reversed in contrast and odd frames are unaltered. It is immediately apparent that the reversed-phi version of the right-translating sinewave is a left-translating sinewave. There is no mystery as to why this stimulus reverses—it is simple algebra.

Figure 4e illustrates five successive frames of van Santen and Sperling's (1984) reversed-phi stimulus. Here, the forward and reverse versions look somewhat different. The dashed lines in Figures 4e and 4f connect the troughs in successive frames. It is obvious that the directions of troughs (and the peaks in between) reverse in the reversed phi stimulus, so the apparent direction should reverse. But it is not obvious that the reversed direction in the reversed-phi stimulus should have exactly the same motion energy as the forward direction in the normal stimulus. This fact is demonstrated in Table 1.

Table 1 analyzes the first 12 terms in the Fourier series expansion of the stimuli in Figures 4e and 4f. It is obvious that in any periodic, 90º-stepping reverse-phi stimulus, the fundamental frequency, the first term in the Fourer expansion, is reversed, and so, too, are all the odd terms in the series. The even terms are also reversed, but they contain no motion information. Thus, for a periodic stimulus that steps 90º in successive frames, reversing the contrast of the even-numbered frames reverses the direction of all the motion energy in the stimulus. Therefore, the mystery in such stimuli is not whether reversed-phi movement is perceived, but how forward movement could be perceived.

For stimuli that are not periodic and do not move exactly 90º in each step, the question of whether forward or reversed motion will be seen following a contrast reversal of even frames is more complex. The Fourier expansion of a reversed-phi stimulus typically involves a complex mixture of partially reversed and unreversed motion components. For reversed-phi and similar stimuli, Dosher, Landy, and Sperling (1989) found that the strength of the first-order stimulus to motion perception was predicted by the ratio of the number of forward-to-backward Fourier components that exceeded a small threshold within the window of visibility (about 30 Hz $\times$ 15 cpd).

Computing the forward direction in reversed phi. Chubb and Sperling (1989b) used a 90º-stepping, contrast-reversing grating (Figures 4f and 5b), rather than merely a contrast-reversing bar (as in the original demonstrations). Chubb and Sperling (1989b) observed that the same stimuli appear to move in the forward direction (the direction of the displacement) when viewed from

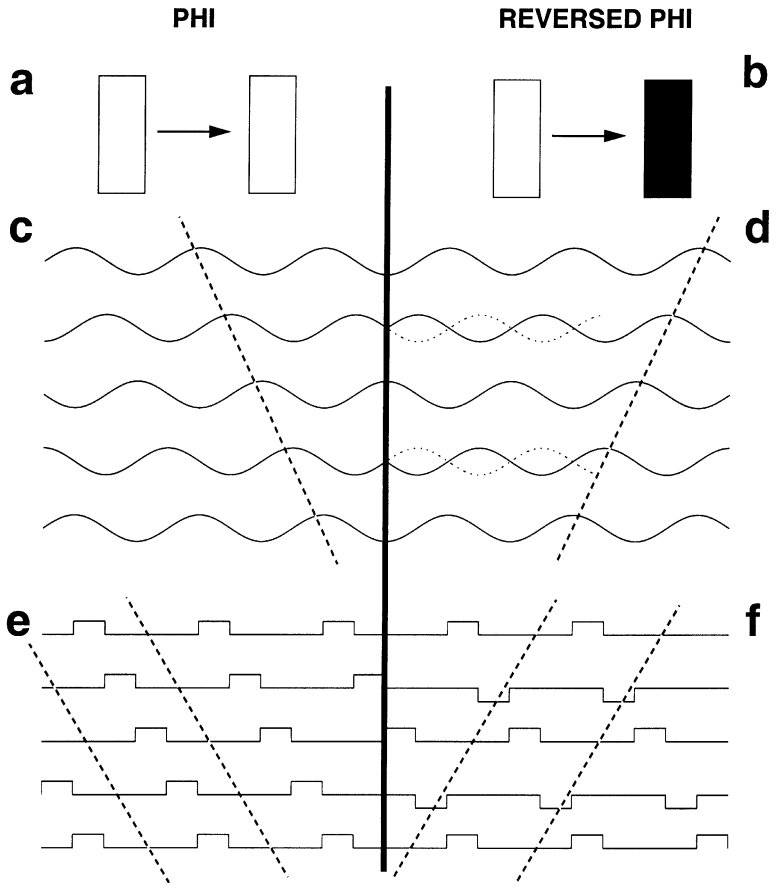

Figure 4. Two frames of (panel a) a normal phi stimulus panel and (b) a reversed-phi stimulus. Panel c: Representation of five frames of a sinewave that translates 90º from frame to frame, as indicated by the dashed line connecting a peak in successive frames. Panel d: Reversed-phi version of the sinewave, in which alternate frames are reversed in sign. The lightly dotted sine indicates the nonreversed frame; the dashed line connects a peak in successive frames. Movement of the reversed-phi sine is exactly opposite to movement of the normal sine. Panel e: A periodic bar stimulus that translates rightward 90º in successive frames. Panel f: Reversed-phi version of panel c. The dashed lines in panels e and f indicate the motion of maxima and minima (fundamental Fourier components) in the two sequences.

near and to move in the reversed direction (opposite to the direction of the displacement) when viewed from afar or in peripheral vision—a finding that has been extensively corroborated in second-order perception (Gorea, 1995; Papathomas & Ramanujan, 1995; Solomon & Sperling, 1995). Chubb and Sperling (1989b) proposed that there exist two motion mechanisms: a first-order mechanism that applies motion energy analysis directly to the *raw* stimulus contrast and a second-order mechanism that applies motion energy analysis to the fullwave-rectified stimulus contrast. The first-order system "perceives" motion in the reversed direction, and it dominates in peripheral vision and for very small stimuli (i.e., when viewing displays from afar). The second-order system "perceives" motion in the forward direction and dominates in near vision. The relative order of dominance, in peripheral or distant viewing, of first- over second- over third-order motion systems) is explained by the relative order of spatial acuity (first- better than second- better than third-order). The first-order system can resolve peripheral stimuli and very small foveal stimuli that are unresolvable by higher orders, and the same is true for the second-order system, relative to the third-order system (Lu & Sperling, 1995b; Solomon & Sperling, 1995).

Figure 5 depicts the Chubb–Sperling contrast-reversing grating and how it is transformed by the presumed fullwave rectification process of their theory. Figure 5a illustrates the simple square-wave of Figure 4e; Figure 5b illustrates the reversed-phi version (as in Figure 4f). Figures 5c and 5d display the raw and the fullwave-rectified version of the Figure 4b reversed-phi stimulus, each with its fundamental Fourier component superimposed. In Figure 5c, motion energy in the leftward direction (indi-

Table 1
Analysis of the Direction of Motion of the Spatial Sinewave Components of Stimuli That Translate Rightward by 90° Steps: Phi (Figure 4e) and Reversed Phi (Figure 4f)

		Phi		Reversed Phi	
Component		Phase Shift*	Direction†	Direction†	Phase Shift*
Fundamental	1	90	→	←	−90
Harmonics	2	180			0
	3	270 = −90	←	→	90
	4	360 = 0			180
	5	450 = 90	→	←	−90
	6	540 = 180			0
	7	630 = −90	←	→	90
	8	720 = 0			180
	9	810 = 90	→	←	−90
	10	900 = 180			0
	11	990 = −90	←	→	90
		⋮			⋮

*The spatial frequency of component n is n times the fundamental frequency; when the fundamental shifts 90°, component n shifts $90n$°. †Components with +90° phase shifts represent motion that is oppositely directed for phi and reversed phi; components with phase shifts of 0° or 180° represent flicker (no motion).

cated by the dominant upper-right to lower-left Fourier component in the display) is much stronger than that in the rightward direction. Thus, motion energy analysis predicts motion in the leftward direction, opposite to the displacement.

To implement *rectification*, a stimulus is defined not in terms of its absolute luminance $l(x,y)$, but in terms of its *point contrast* $c(x,y)$, the normalized deviation of the luminance at each point from the mean luminance $l_o(x,y)$ of the stimulus:

$$c(x,y) = \frac{l(x,y) - l_o(x,y)}{l_o(x,y)}. \quad (1)$$

Fullwave rectification denotes any monotonically increasing function of the absolute value of *point contrast*. Here, fullwave rectification is understood to be the absolute value itself or the square (energy or power), although other functions are possible. Fullwave rectification maps equal positive and negative point contrasts into identical positive values; only the magnitude, not the sign, of the point contrast matters. Thus, fullwave rectification maps deep black and bright white into a large positive value (represented as white), and the mean luminance value (zero point contrast) into zero (represented as middle gray). Motion energy analysis applied to the rectified stimulus (Figure 5d) predicts rightward motion. This is indicated by the slant of the fundamental Fourier component from upper left to lower right in Figure 5d. With appropriate assumptions about the relative spatial frequency sensitivities of the first-order and second-order motion systems in central and peripheral vision (see, e.g., Solomon & Sperling, 1995), this theory easily accounts for reversed-phi phenomena.

The contrast-reversing grating of Figure 5b offers a useful mathematical property for discriminating between fullwave and halfwave rectification in reversed phi. Halfwave rectification is analogous to the processing of *on* and *off* cells in early vision. Halfwave rectification can be either positive (in which case, positive inputs are transmitted, but negative inputs are mapped into zero) or negative (in which case, the sign of negative inputs is reversed, but positive inputs are mapped into zero). Positive or negative halfwave rectification would render the contrast-reversing grating of Figure 5b invisible to motion energy analysis, whereas fullwave rectification is ideal for subsequent extraction of the forward motion (Chubb & Sperling, 1989b). That forward motion is easily perceived means that halfwave rectification is not necessary for second-order motion perception (the forward movement in first-order reversed phi) and that fullwave rectification is sufficient. In a related study, Solomon and Sperling (1994) show that halfwave rectification is vastly insufficient as an account for second-order motion perception.

To summarize, studies of the reversed-phi phenomenon demonstrate that there exist two motion systems. The first-order system applies a motion energy computation directly to raw stimulus contrast; the second-order system extracts motion from fullwave-rectified stimulus contrast. However, the motion algorithm by which the second-order system computes motion cannot be deduced from these experiments. The second-order reversed-phi paradigm (detailed below) offers a way to determine the second-order motion algorithm.

Second-order reversed phi. To test whether motion energy analysis is the algorithm ultimately used by the human visual system to extract motion from second-order motion stimuli, we created a class of stimuli (Figure 6) that we called *second-order reversed-phi* stimuli, to distinguish them from the earlier reversed-phi stimuli (Anstis, 1970; Anstis & Rogers, 1975; Chubb & Sperling, 1989b), which probably should now be called first-order reversed-phi stimuli. All the second-order reversed-phi stimuli tested herein have the following property: After linear spatiotemporal filtering and fullwave rectification, they become equivalent to the first-order reversed-phi stimuli used by Chubb and Sperling (1989b). There are two advantages to using a contrast-reversing grating rather than a contrast-reversing bar: (1) The grating has a much narrower spatial frequency content than does a bar and, therefore, is more useful when spatial frequency is to be manipulated; (2) the contrast-reversing grating is ambiguous following halfwave rectification. Therefore, the ability to detect grating motion (or equivalently, the ability to detect grating orientation in the x,y version) implies that the second-order process uses fullwave (vs. halfwave) rectification.

Figure 6 shows three displays that are candidates for yielding perceptual second-order reversed phi. In each display, there is a neutral background texture that occupies 75% of the display area. The remaining 25% of the stimulus is filled with a textured rectangle that varies from frame to frame in texture contrast (Figure 6a), in texture spatial frequency (Figure 6b), or in temporal frequency (i.e., flicker rate; Figure 6c).

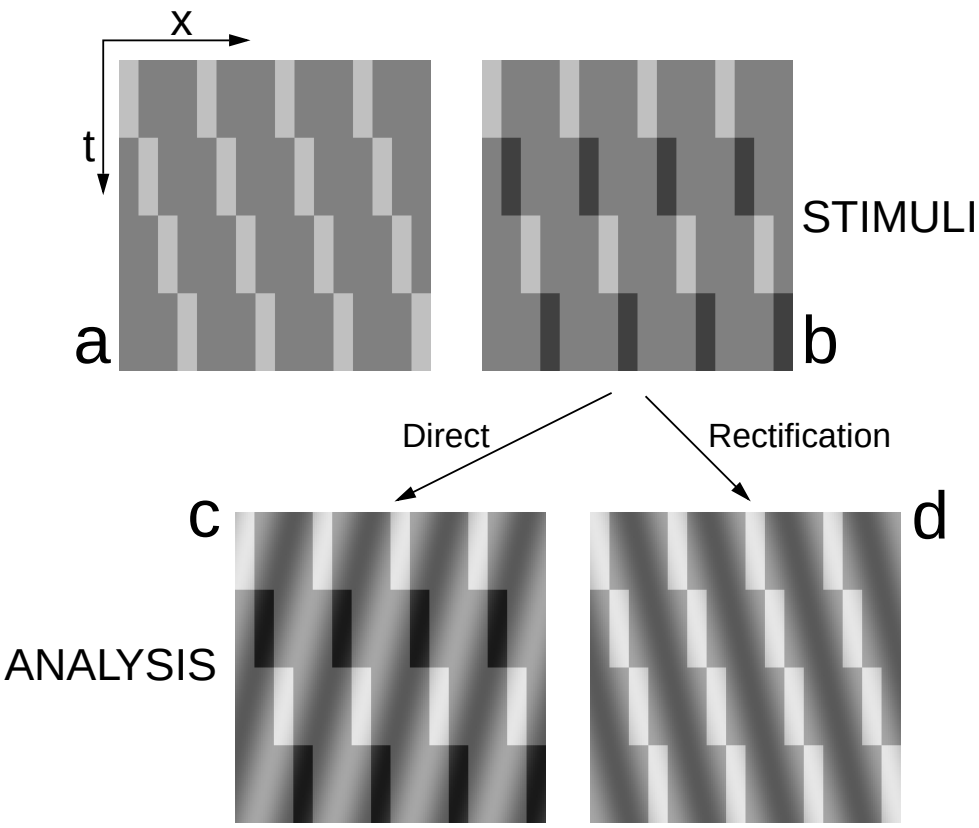

Figure 5. First-order reversed-phi: stimulus and theory. The horizontal axis represents space; the vertical axis represents time. Panel a: Four frames of a first-order reversed-phi stimulus (Chubb & Sperling, 1989a), in which the contrast of the bars alternates polarity (from white to black and from black to white) from frame to frame. Panel b: Direct computation. Applying motion energy analysis directly to raw stimulus contrast predicts motion direction that is opposite to the bar displacement (*reversed* phi) because the dominant Fourier component (indicated by the light and the dark stripes of a superimposed sinewave grating) is oriented in the leftward direction. In viewing in the periphery or from afar, human observers perceive this so-called reversed motion direction (as predicted by motion energy analysis.) Panel c: In central vision, humans perceive motion in the forward direction, contradicting what is predicted by motion energy analysis. This is explained by a model in which stimulus point contrast is first fullwave rectified (absolute value computation) and only then subjected to motion energy analysis. After rectification, the dominant Fourier component is in the forward direction (indicated by the superimposed sinewave grating).

Second-order texture contrast stimulus. In Figure 6a, the textured rectangle increases and decreases its texture contrast, relative to the background in alternate frames. For the second-order system, increasing and decreasing texture contrast is equivalent to increasing and decreasing luminance in the first-order system (Chubb & Sperling, 1988; Chubb, Sperling, & Solomon, 1989). The stimulus of Figure 6a is similar to the stimulus of Nishida (1993) in the only previous published observation of second-order reversed phi. A "window" through which a check pattern is visible is translated from frame to frame. Nishida's stimulus involved just two levels of texture contrast; the areas to which these contrast levels were assigned alternated in consecutive frames. The stimulus in Figure 6a involves three levels of texture contrast, the middle level remaining the same from frame to frame and the areas of high and low contrast reversing on consecutive frames. Nishida inferred from his observations that second-order reversed phi used a correlation mechanism (after rectification) similar to first-order motion mechanisms; he did not consider how the forward motion might be computed.

Second-order spatial frequency stimulus. The textures in Figures 6b and 6c are novel. In Figure 6b, the spatial frequency of the texture of the remaining rectangles alternately increases and decreases (relative to the background) in successive frames. In second-order motion, decreasing spatial frequency is equivalent to increasing texture contrast (Werkhoven, Sperling, & Chubb, 1993, 1994), so these stimuli, too, become reversed-phi stimuli for the second-order system.

Second-order flicker stimulus. Figure 6c represents flickering stimuli. The background has a flicker rate intermediate between the alternating high and low flicker rates of the translating rectangle.

Analysis of the second-order reversed-phi stimuli. The stimuli of Figures 6a, 6b, and 6c are preprocessed by

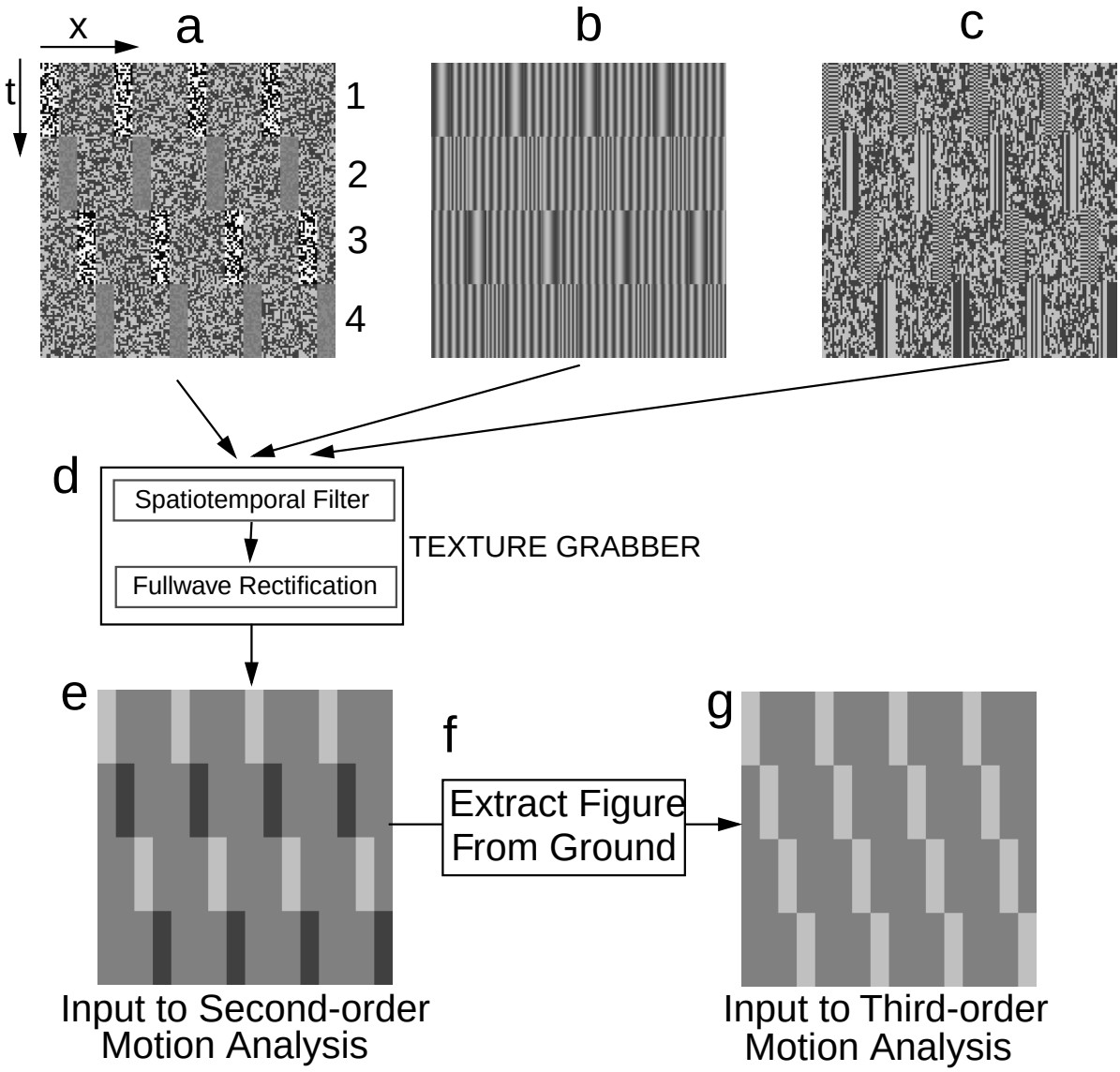

Figure 6. Second-order reversed-phi: stimuli and analysis. The horizontal axis represents space. Panels a and b show four consecutive frames as viewed by the observer. Panel a: Contrast modulation. The translating bars are composed of either high-contrast texture (point contrast = ±0.94) or low-contrast texture (point contrast = ±0.06) on a medium-contrast background (point contrast = ±0.50). In successive frames, the texture bars move one bar width to the right, and the high-contrast regions switch to low contrast, and vice versa. Panel b: Spatial frequency modulation. The bars are composed of either low-spatial-frequency (2.36 cpd) sinewave gratings or high-spatial-frequency (9.44 cpd) sinewave gratings on a medium-spatial-frequency (4.72 cpd) sinewave grating background. The bars shift one bar width to the right and alternate between high- and low-spatial-frequency textures in successive frames, always with a new random spatial phase. Panel c: Flicker modulation. The vertical axis represents time. All the stimuli are composed entirely of vertical stripes; the *x*,*t* graph represents the color of a stripe at a particular instant in time. For the first- and third-quarter cycles of the stimulus (rows 1 and 3), the bars represent regions with a maximum rate of pixel flicker (a black–white reversal of every pixel on every frame), superimposed on a background that has a random, medium rate of flicker. In the second- and fourth-quarter cycles, bars remain unchanged during their entire exposure (vertical stripes in panel c, low flicker rate regions). The translating bars displace one bar width to the right, switching from high to low flicker and vice versa from frame to frame. Panels d and e: Spatiotemporal filtering and fullwave rectification (see Figure 3). Panel f: The output of the fullwave rectifier for any of the stimuli a, b, or c can be represented as a space–time graph. For stimuli a and b, panel f can be also be interpreted as representing four consecutive frames of texture grabber output. The dominant motion energy in panel f is leftward (opposite to the bar displacement direction). Applying motion energy analysis on the output of the texture grabber would predict motion in the reversed direction. A salience system that marked the location of features that differed from the background in each frame would compute motion in the forward direction.

a *texture grabber* (Figure 6d) that consists of a low-pass spatial filter and a band-pass temporal filter followed by fullwave rectification. The texture grabber produces an output that is equivalent to a first-order reversed-phi stimulus. Rectification alone would have sufficed to reveal the second-order motion of the texture contrast modulation stimulus in Figure 6a. However, rectification must be proceeded by low-pass spatial filtering, to expose the motion of the three-grating-frequencies stimulus of Figure 6b. Temporal band-pass or temporal low-pass filtering followed by rectification is required to expose the motion of the flicker stimulus of Figure 6c (Chubb & Sperling, 1988).

Figure 6f illustrates that, after preprocessing, the dominant motion energies of the reversed-phi stimuli of Figures 6a, 6b, and 6c are in the leftward direction, *opposite* to the rightward displacement of the bars. The motion that is extracted from second-order reversed-phi stimuli by a texture grabber, followed by a motion energy computation, would be *reversed* motion. On the other hand, the third-order motion mechanism extracts the location of the most salient stimulus features in each frame (the figure) and computes motion on the basis of the spatiotemporal movement of these locations (Lu & Sperling, 1995a; Smith, 1994). Third-order motion is in the rightward (forward) direction. Therefore, there may be conditions under which motion is seen in the forward direction.

Our aim here is to find conditions under which second-order reversed-phi stimuli are perceived in the reversed direction, because this is a necessary condition for the second-order motion theory proposed by Chubb and Sperling (1988). If there were a second-order motion energy mechanism, it must manifest itself, and second-order reversed phi would be one obvious manifestation. On the other hand, perceiving second-order reversed-phi stimuli in the forward direction would be consistent with the third order motion computation proposed by Lu and Sperling (1995a). We expect that, if third-order motion is perceived, it would be perceived at low temporal frequencies and in central vision, because Lu and Sperling (1995b) found that the third order (salience motion) mechanism has a much lower cutoff frequency (at 3 Hz) than does the motion energy system and it has coarser spatial resolution. Indeed, previous stimuli that were constructed to evade the first-order motion system (and that probably stimulated a combination of second- and third-order motion) have been found to require lower temporal and spatial frequencies than do first-order stimuli (Anstis, 1974; Millodot, Johnson, Lamont, & Leibowitz, 1975; Weymouth, 1958). So, in appropriately chosen viewing conditions (fovea, low temporal frequencies), it might be possible for the third-order system to dominate the motion extraction process.

METHOD

Stimuli

Three kinds of second-order four-frame displays were generated: contrast modulation (Figure 6a), spatial frequency modulation (Figure 6b), and flicker modulation (Figure 6c). They all share the following principle: After linear spatiotemporal filtering and fullwave rectification (Figure 3), they resemble the reversed-phi stimuli (Figure 5a) used by Chubb and Sperling (1989b).

All the stimuli are periodic in space, each spatial period consisting of four adjacent areas, called *vertical bars*. The vertical bars are filled with textures as follows. Let i denote the horizontal location of a bar ($i = 0, 1, 2, \ldots$), j denote the frame number ($j = 0, 1, 2, 3$), $p[i]$ denote the property of bar i, and H, M, and L denote high, medium, and low amplitudes of the second-order texture or flicker. All three kinds of displays are described by the following logic statements:

$$\text{if } [(i \bmod 4 = j) \text{ and } (j \bmod 2 = 0)], \quad (2a)$$

$$p[i] = H;$$

$$\text{else if } [(i \bmod 4 = j) \text{ and } (j \textit{ mod } 2 = 1)], \quad (2b)$$

$$p[i] = L;$$

$$\text{else}$$

$$p[i] = M. \quad (2c)$$

Contrast modulation stimulus. The bars are filled with pixels (3.2 min × 3.2 min) that are randomly black or white—the carrier texture. $p[i]$ defines the point contrast of the bars: $H = \pm 0.94$, $M = \pm 0.50$, and $L = \pm 0.06$. The width of each bar extends 0.424º (8 pixels). The carrier texture remains the same from frame to frame; only its contrast is varied.

Spatial frequency modulation stimulus (texture quilt; Chubb & Sperling, 1991). The spatial frequency of vertical gratings that occupy each bar (width = 0.424º) is defined by $p[i]$, where $H =$ 9.44 cpd, $M = 4.72$ cpd, and $L = 2.36$ cpd. The highest frequency grating is a square wave; the others are the best possible approximations to a sinewave. The peak point contrast of the sinewaves was fixed at 0.50. In successive frames, a new different random phase was used for the grating in every bar.

Flicker rate modulation stimulus. The stimulus was made of random black–white pixels (3.2 min × 3.2 min). The probability that a pixel would change the sign of its point contrast from frame to frame is given by $p[i]$, where $H = 1$, $M = 0.30$, and $L = 0$. The background flicker rate, $M = 0.3$, was chosen to be perceptually intermediate between the lowest and the highest flicker rates, $L = 0$ and $H = 1$. (The apparatus produced 60 refreshes per second; every successive pair of these was identical and is called a frame; 30 frames were presented each second.) Thus, the highest flicker rate was 15 Hz, the lowest 0 Hz, and the background was made up of the whole spectrum of intermediate flicker rates.

All the displays extended 6.80º × 6.80º, centered in a uniform background extending to 19.6º × 12.9º. The average luminance of objects in the room was about 10 cd/m^2. To remove edge effects, the contrast of the displays was multiplied by a spatial Gaussian window. Let x and y (in degrees) denote the horizontal and the vertical distances from the center of the display, and let $\sigma = 2.54$º denote the standard deviation of the Gaussian function. The window is described as

$$g(x, y) = \exp\left(\frac{1}{2\sigma^2}(x^2 + y^2)\right).$$

Apparatus

All the stimuli were created off line, using the HIPS image-processing software on a SUN Sparc 2 computer (Landy, Cohen, & Sperling, 1984a, 1984b). The stimuli were transmitted to an IBM 486 PC-compatible computer through PC NFS (Sun Microsystems) and presented on a 20-in. diagonal, 60-Hz vertical retrace IKEGAMI DM516A monochrome graphics monitor with a fast, white P4-type phosphor. The display was controlled by an AT-Vista

video graphics board driven by programs on the PC (Hall & Gegenfurtner, 1988). The display system (AT-Vista board plus IKEGAMI monitor) had a sufficiently extended temporal frequency response so that it produced no measurable horizontal pixel interactions on the monitor.

A psychophysical procedure was used to generate an 8-bit linear lookup table that mapped the 4,096 different voltage in the display system to 255 equal-step gray levels.[3] The lowest [$L(1)$], highest [$L(255)$], and middle [$L(128)$] display luminances were, respectively, $L(1) = 12.1$ cd/m^2, $L(255) = 325$ cd/m^2, and $L(128) = [L(1) + L(255)] / 2.0 = 169$ cd/m2. L(128) was used throughout as the mean background luminance level. Considerable care was taken to ensure that the stimuli actually produced on the monitor were exactly the same as the stimuli described in the text.

Procedure

To change the relative strength of the second-order motion energy system and the third-order (salience) motion system (Lu & Sperling, 1995b; Pantle, 1992; Papathomas & Ramanujan, 1995; Smith, Hess, & Baker, 1994; Solomon & Sperling, 1995), we manipulated the temporal frequency of the stimuli (reciprocal of the time for one complete cycle) and also the viewing conditions (central vs. peripheral vision). In an experimental session, the observer was asked either to fixate at the center of the monitor or to fixate at a point that was about 5º off to the side (alternating left or right in different trials) of the center. After observing the stimulus, the observer was asked to report the perceived motion direction. This was repeated several times with different directions of the presented motion stimulus. In 90 of 96 conditions, the direction of motion was perfectly obvious and not at all ambiguous, so more elaborate procedures were not needed. In 6 of the 96 conditions (stimulus × observer × eccentricity), there was some degree of subjective ambiguity about motion direction. In these cases, 15 trials were conducted to determine the fraction of presentations in which a motion direction was perceived in the forward or the reversed direction.

All the stimuli consisted of precisely one cycle; the duration was 1 / (temporal frequency). Five different temporal frequencies (0.94, 1.88, 3.75, 7.50, and 15 Hz, equivalent to velocities of 1.59, 3.19, 6.36, 12.7, and 25.4 deg/sec) were used for the moving contrast modulation stimulus (Figure 6a). Because of equipment constraints on the presentation rate as a function of the complexity of frames, only the four lowest temporal frequencies (0.94, 1.88, 3.75, and 7.50 Hz) were used for the spatial frequency modulation stimulus. For the flicker stimulus (Figure 6c), the interactions between flicker frequency (which defined the bars) and modulation frequency (which defined the movement) produced great perceptual ambiguity at high motion modulation frequencies, so only the three lowest velocities (temporal movement frequencies 0.94, 1.88, and 3.75 Hz) were used.

Observers

Three UCI graduate students, naive to the purposes of the experiment, and the first author served as observers for the full range of conditions. All the subjects, 3 males and 1 female, were in their twenties. In addition, 3 other observers viewed some of our displays. All the observers had normal or corrected-to-normal vision.

RESULTS

Peripheral Vision

In peripheral vision, every observer saw presentations only in the *reversed* direction (opposite to the bar displacement). In some conditions—for example, at the highest temporal frequencies of the flicker modulation stimuli—there were some trials on which no motion was perceived. When motion was perceived, however, it was universally in the direction of second-order reversed phi.

Table 2
Perceived Motion Direction of Second-Order Reversed-Phi Stimuli

Stimulus Type	Temporal Frequency (Hz)	Subject							
		Z.L.		D.M.		S.R.		E.B.	
		0º	5º	0º	5º	0º	5º	0º	5º
Contrast modulation	0.94	F	R	F	R	F	R	F	R
	1.88	F	R	F	R	F	R	F	R
	3.75	F	R	F	R	F	R	F	R
	7.5	R(.65)	R	F(.65)	R	R(.70)	R	F(.70)	R
	15.0	R	R	R	R	R	R	R	R
Spatial frequency modulation	0.94	F	R	F	R	F	R	F	R
	1.88	F	R	F	R	F	R	F	R
	3.75	R	R	R	R	R	R	R	R
	7.50	R	R	R	R	R	R	R	R
Flicker modulation	0.94	F	R	F	R	F	R	F	R
	1.88	F	R	F	R	F	R	F	R
	3.75	R	R	R(.70)	R	R	R	R(.70)	R

Note—0º, central vision; 5º, peripheral vision; F, forward motion direction; R, reversed motion direction. The numbers in the brackets following F or R indicate that the fraction motion was perceived in that direction. F or R without brackets indicates that motion was perceived in that direction all the time.

Central Vision

In central viewing, the observers reported perceiving motion in the forward direction at low temporal frequencies and in the reversed direction at high temporal frequencies (Table 2). The temporal frequency at which the direction of perceived motion changed depended on the stimulus, but was similar for all the observers.

Contrast modulation. In central vision, all the observers perceived motion in the reversed direction at 15 Hz and motion in the forward direction at temporal frequencies of 0.94, 1.88, and 3.75 Hz. 7.5 Hz was ambiguous for all the observers.

Spatial frequency modulation. In central vision, all the observers reported forward motion at temporal frequencies of 0.94 and 1.88 Hz and reversed motion at 3.75 and 7.50 Hz.

Flicker modulation. In central vision, at temporal frequencies of 0.94 and 1.88 Hz, all the observers reported perceiving motion in the forward direction. At the highest reasonable temporal frequency for these stimuli (3.75 Hz), all the motion reports of all the observers were in the reversed direction. Observers D.M. and E.B. reported that they could only perceive motion about 70% of the time. However, whenever they did perceive motion, it occurred in the reversed direction.

In informal observations, we noticed that moving the observer away from the displays had the same effect as changing from central viewing to periphery viewing: Reversed motion became more dominant. The 3 unofficial observers, who viewed only some of the displays, all saw

only reversed motion in peripheral viewing. Indeed, every observer who has viewed these displays has been able to perceive second-order reversed-phi motion and has perceived only reversed-phi motion in peripheral vision.

DISCUSSION

The Mechanisms of Second-Order Reversed Phi

The perception of first-order reversed phi in the Chubb–Sperling contrast-reversing grating is a property of the motion energy algorithm—indeed, of any algorithm that computes Fourier motion energy (Table 1). In the analysis of second-order reversed-phi stimuli, the texture grabber (Figure 3) transforms each of the three second-order reversed-phi stimuli into the equivalent of a first-order reversed-phi Chubb–Sperling grating. That is, in the three second-order reversed-phi stimuli, texture grabbers produce greater outputs in areas that contain higher contrasts, lower spatial frequency gratings, or higher flicker rates. As in the first-order Chubb–Sperling contrast-reversing grating, most of the motion energy, then, is in the reversed direction. Of course, the stimuli were constructed to be consistent with this hypothesized texture grabber. That humans perceive motion in the reversed direction when viewing these second-order reversed-phi stimuli supports both the hypothesis of the texture grabber preprocessing and that of (Fourier) motion energy analysis (e.g., Figure 3) as being the mechanism of human second-order motion analysis.

The Mechanisms of Perceived Forward Motion in Second-Order Reversed-Phi Stimuli

Because the second-order reversed-phi stimuli are invisible to first-order analysis,[4] and because second-order analysis produces motion in the reversed direction, the perception of forward motion requires yet another mechanism, presumably the third-order salience map mechanism proposed by Lu and Sperling (1995a).

The three reversed-phi stimuli in our experiments were constructed so that one fourth of the area was occupied by the *figure*, which changed type from frame to frame, and three fourths of the area was occupied by the *background*, which remained physically unchanged from frame to frame in the contrast modulation stimuli and unchanged in type for the spatial frequency and flicker stimuli. The third-order motion mechanism is assumed by Lu and Sperling (1995a) to compute the moment-to-moment motion of those parts of the visual stimulus that are marked as figure in a neural salience field. So, if (1) occupying a small part of the field and changing from frame to frame were to cause that portion of the stimulus to be marked as figure, and (2) occupying a large part of the field and remaining stable were to cause that portion of the stimulus to be marked as ground, and (3) the third-order motion system computed the motion of figure, then the second-order reversed-phi stimuli would support third-order motion in the forward direction. This is precisely what occurred.

Third-order motion has a much lower frequency cutoff (≈3–4 Hz) than does second-order motion (≈10–12 Hz; Lu & Sperling, 1995b). Similarly, the higher the order of the motion system, the lower is its spatial resolution, and therefore, the more likely it is to be confined to areas near the fovea, where spatial frequency resolution is better. These results—that the third-order motion direction was (1) never perceived in peripheral viewing and (2) perceived in foveal areas only at low temporal frequencies—are entirely consistent with the previously noted properties of motion systems.

Past and Future Observations

The changeover from perceived second-order reversed direction to third-order forward direction occurred at different temporal frequencies for the three second-order reversed-phi stimuli. The changeover frequency depends on the relative strength of the second-order and third-order components of the stimuli; in the absence of fully specified models for second- and third-order motion, quantitative predictions of changeover frequency are impossible. However, the narrow range of ambiguity (in which one of two oppositely directed motions fails to dominate completely) is quite consistent with earlier reports of motion competition (Burt & Sperling, 1981). Perceiving ambiguity in motion appears not to be of evolutionary value.

To determine whether the so-called second- and third-order mechanisms that support reversed and forward motion, respectively, in the stimuli of this study are the same mechanisms as those reported by Lu and Sperling (1995b) would require additional observations. For example, these authors found the second-order mechanisms to be entirely monocular, whereas the third-order mechanism was indifferent to whether successive frames of the stimulus were received in the same or in alternating eyes. Some of the present stimuli could be tested for sensitivity to interocular versus monocular presentation. And the actual temporal frequency tuning functions for stimuli like those in the present experiments could be measured, to determine how closely they agree with previously measured tuning functions.

Finally, in addition to reversed-phi motion based on texture grabber output and third-order motion based on relative areas of figure and ground, there are other aspects of the stimuli that could be used to compute motion direction. Consider, for example, frame-to-frame transitions. Between frames, in the contrast-modulated stimulus, the one fourth of the stimulus that has different contrast from the remainder returns to background level, whereas the adjacent one fourth of the stimulus increases or decreases its contrast. In all these cases, some pixels increase intensity or point contrast, and an expected equal number of pixels decrease. Insofar as the temporal filters of texture grabbers respond to these changes of point contrast and their output is rectified, this would produce a motion component in the forward (not the reversed-phi) direction. However, there is no reason to suppose

that such an output of texture grabbers would exhibit the temporal frequency and the central–peripheral viewing differences that distinguish the forward and reversed-phi directions.

Although a frame-to-frame transition-sensitive mechanism might report motion in the forward direction for the contrast-modulated second-order phi stimulus, for the spatial frequency modulated stimulus, a transition mechanism would fail to report any motion direction, because there are approximately equal frame-to-frame changes at all the stimulus locations. For the flicker stimuli, it is not obvious how a transition-sensitive mechanism would operate when pixel changes occur everywhere throughout all the frames. Thus, although it is not yet certain which of several conceivable computations are actually used by second-order, third-order, or, perhaps, other motion systems, only two biologically plausible mechanisms that we know of that would extract forward motion from all three reversed-phi stimuli: (1) selecting as figure homogeneous areas that are relatively smaller than their surround, and (2) selecting areas of relatively greater activity.

In conclusion, we tentatively identify the mechanism that computes motion in the second-order reversed-phi direction as a motion energy computation on the output of texture grabbers and the mechanism that computes forward motion as a third-order motion energy computation on the output of a figure–ground computation (as embodied in a salience map).

REFERENCES

Adelson, E. H., & Bergen, J. K. (1985). Spatio-temporal energy models for the perception of apparent motion. *Journal of the Optical Society of America A*, **2**, 284-299.

Anstis, S. M. (1970). Phi movement as a subtraction process. *Vision Research*, **10**, 1411-1430.

Anstis, S. M. (1974). A chart demonstrating variations in acuity with retinal position. *Vision Research*, **14**, 589-592.

Anstis, S. M., & Rogers, B. J. (1975). Illusory reversal of visual depth and movement during changes of contrast. *Vision Research*, **15**, 957-961.

Burt, P., & Sperling, G. (1981). Time, distance, and feature trade-offs in visual apparent motion. *Psychological Review*, **88**, 171-195.

Cavanagh, P., & Mather, G. (1989). Motion: The long and the short of it. *Spatial Vision*, **4**, 103-129.

Chubb, C., & Sperling, G. (1988). Drift-balanced random stimuli: A general basis for studying non-Fourier motion perception. *Journal of the Optical Society of America A*, **5**, 1986-2006.

Chubb, C., & Sperling, G. (1989a). Second-order motion perception: Space–time separable mechanisms. In *Proceedings: Workshop on visual motion* (pp. 126-138). Washington DC: IEEE Computer Society Press.

Chubb, C., & Sperling, G. (1989b). Two motion perception mechanisms revealed by distance driven reversal of apparent motion. *Proceedings of the National Academy of Sciences*, **86**, 2985-2989.

Chubb, C., & Sperling, G. (1991). Texture quilts: Basic tools for studying motion-from-texture. *Journal of Mathematical Psychology*, **35**, 411-442.

Chubb, C., Sperling, G., & Solomon, J. A. (1989). Texture interactions determine perceived contrast. *Proceedings of the National Academy of Sciences*, **86**, 9631-9635.

Derrington, A. M., & Badcock, D. R. (1985). Separate detectors for simple and complex grating patterns? *Vision Research*, **25**, 1869-1878.

Dosher, B. A., Landy, M. S., & Sperling, G. (1989). Kinetic depth effect and optic flow: 1. 3D shape from Fourier motion. *Vision Research*, **29**, 1789-1813.

Emerson, R. C., Bergen, J. R., & Adelson, E. H. (1992). Directionally selective complex cells and the computation of motion energy in cat visual cortex. *Vision Research*, **32**, 203-218.

Exner, S. (1875). Über das Sehen von Bewegungen und die Theorie des zusammensetzen Auges. *Sitzungsbericht Akademie Wissenschaft (math.-naturw.)*, **72**, 156-190.

Gorea, A. (1995). Spatiotemporal characterization of a Fourier and non-Fourier motion system. *Vision Research*, **35**, 907-914.

Hall, P., & Gegenfurtner, K. (1988). *Run-Time Library, The HIPL picture processing software*. New York: New York University, Psychology Department, Human Information Processing Laboratory. University.

Knutsson, H., & Granlund, G. H. (1983). Texture analysis using two-dimensional quadrature filters. In *1983 IEEE Computer Society workshop on computer architecture for pattern analysis and image database management* (pp. 206-213). Washington, DC: IEEE Computer Society Press.

Landy, M. S., Cohen, Y., & Sperling, G. (1984). HIPS: Image processing under UNIX. Software and applications. *Behavior Research Methods, Instruments, & Computers*, **16**, 199-216.

Landy, M. S., Cohen, Y., & Sperling, G. (1984b). HIPS: A Unix-based image processing system. *Computer Vision, Graphics & Image Processing*, **25**, 331-347.

Lelkins, A. M. M., & Koenderink, J. J. (1984). Illusory motion in visual displays. *Vision Research*, **24**, 293-300.

Lu, Z.-L., & Sperling, G. (1995a). Attention-generated motion perception. *Nature*, **377**, 237-239.

Lu, Z.-L., & Sperling, G. (1995b). The functional architecture of human visual motion perception. *Vision Research*, **35**, 2697-2722.

Lu, Z.-L., & Sperling, G. (1996a). Contrast gain control in first- and second-order motion perception. *Journal of the Optical Society of America A*, **13**, 2305-2318.

Lu, Z.-L., & Sperling, G. (1996b). *The existence of second-order reversed phi: A prediction from a theory of motion perception* (Tech. Rep. MBS 96-01, pp. 1-6). University of California, Irvine, Institute of Mathematical Behavioral Sciences.

Lu Z.-L., & Sperling, G. (1996c). The three mechanisms of human visual motion detection. *Current Directions in Psychological Science*, **5**, 44-53.

Lu, Z.-L., & Sperling, G. (1999). The amplification principle in motion perception [Abstract]. *Investigative Ophthalmology & Visual Science*, **40** (4), S199.

Millodot, M., Johnson, C. A., Lamont, A., & Leibowitz, H. A. (1975). Effect of dioptrics on peripheral visual acuity. *Vision Research*, **15**, 1357-1362.

Nishida, S. (1993). Spatiotemporal properties of motion perception for random-check contrast modulations. *Vision Research*, **33**, 633-645.

Pantle, A. (1992). Immobility of some second-order stimuli in human peripheral vision. *Journal of the Optical Society of America A*, **9**, 863-867.

Papathomas, T. V., & Ramanujan, K. S. (1995). Grouping in sparse reverse-contrast static flow (glass) patterns. *Investigative Ophthalmology & Visual Science*, **36** (ARVO Suppl., 477).

Ramachandran, V. S., Rao, M. V., & Vidyasagar, T. R. (1973). Apparent movement with subjective contours. *Vision Research*, **13**, 1399-1401.

Reichardt, W. (1961). Autocorrelation, a principle for the evaluation of sensory information by the central nervous system. In W. A. Rosenblith (Ed.), *Sensory communication* (pp. 303-317). New York: Wiley.

Smith, A. T. (1994). Correspondence-based and energy-based detection of second-order motion in human vision. *Journal of the Optical Society of America A*, **11**, 1940-1948.

Smith, A. T., Hess, R. F., & Baker, C. L. (1994). Direction identification thresholds for second-order motion in central and peripheral vision. *Journal of the Optical Society of America A*, **11**, 506-514.

Solomon, J. A., & Sperling, G. (1994). Full-wave and half-wave rectification in second-order motion perception. *Vision Research*, **34**, 2239-2257.

Solomon, J. A., & Sperling, G. (1995). 1st- and 2nd-order motion and texture resolution in central and peripheral vision. *Vision Research*, **35**, 59-64.

Sperling, G. (1976). Movement perception in computer-driven visual displays. *Behavior Research Methods & Instrumentation*, **8**, 144-151.

Sperling, G., & Lu, Z.-L. (1996). Second-order reversed-phi reveals two mechanisms: Second-order motion energy and third-order feature salience. *Investigative Ophthalmology & Visual Science*, **37**(ARVO Suppl.), S900.

Turano, K., & Pantle, A. (1989). On the mechanism that encodes the movement of contrast variations: Velocity discrimination. *Vision Research*, **29**, 207-221.

van Santen, J. P. H., & Sperling, G. (1984). Temporal covariance model of human motion perception. *Journal of the Optical Society of America A*, **1**, 451-473.

van Santen, J. P. H., & Sperling, G. (1985). Elaborated Reichardt detectors. *Journal of the Optical Society of America A*, **2**, 300-321.

Victor, J. D., & Conte, M. M. (1990). Motion mechanisms have only limited access to form information. *Vision Research*, **30**, 289-301.

Watson, A. B., & Ahumada, A. J., Jr. (1983). A look at motion in the frequency domain. In J. K. Tsotsos (Ed.), *Motion: Perception and representation* (pp. 1-10). New York: Association for Computing Machinery. (Also published as NASA Technical Memorandum 84352).

Watson, A. B., Ahumada, A. J., Jr., & Farrell, J. E. (1986). Window of visibility: A psychophysical theory of fidelity in time-sampled visual motion displays. *Journal of the Optical Society of America A*, **3**, 300-307.

Werkhoven, P., Sperling, G., & Chubb, C. (1993). The dimensionality of texture-defined motion: A single channel theory. *Vision Research*, **33**, 463-485.

Werkhoven, P., Sperling, G., & Chubb, C. (1994). Perception of apparent motion between dissimilar gratings: Spatiotemporal properties. *Vision Research*, **34**, 2741-2759.

Wertheimer, M. (1912). Experimentelle Studien über das Sehen von Bewegung. *Zeitschrift für Psychologie*, **61**, 161-265.

Weymouth, F. W. (1958). Visual sensory units and the minimum angle of resolution. *American Journal of Ophthalmology*, **46**, 102-113.

Zhou, Y. X., & Baker, C. L., Jr. (1993). A processing stream in mammalian visual cortex neurons for non-Fourier responses. *Science*, **261**, 98-101.

NOTES

1. Even though different theories may compute the same algebraic quantities in terms of overall system input–output, they may suggest quite different neural implementations of this computation (e.g., Emerson, Bergen, & Adelson, 1992).

2. A preliminary account of this research appeared in Sperling and Lu (1996) and Lu and Sperling (1996b).

3. The aim of a calibration procedure is to determine the look-up table value, so that a requested intensity is accurately produced by the graphics display hardware. Although only 256 different intensities (8 bits) can be displayed within a single frame, specially designed local hardware permits pixel intensities to be designated with an accuracy of 1/4,096 (12 bits). The calibration procedure determines which subset of the 4,096 available requested outputs will produce the 256 most evenly spaced values. The procedure for producing such a linear look-up table, which has been in use in the second author's laboratory for over 20 years, involves creating, in one area of the viewing surface, as uniform as possible a mixture (in space and time) of equal quantities of zero- and full-intensity pixels and determining the look-up table value of pixels in an adjacent homogeneous area (in which all the pixels have the same intensity) that produces a psychophysical match to the luminance of the mixed-pixel area. The first match determines the look-up table value for 0.5 of maximum luminance. A mixture of 0.5 and 1 pixels is used to determine the ¾ value, and this procedure is repeated until seven values from ⅛ to ⅞ have been determined. These matches are repeated, and various checks for consistency are made, such as verifying that a mixture of ¾ and ¼ matches 0.5. The remaining look-up table values are derived from the first nine values by means of an a priori functional form (gamma power function), a spline, or a linear interpolation, as appropriate. The procedure is repeated at regular intervals, to ensure that calibration remains valid. The particular display monitor used in these experiments (IKEGAMI DM516A monochrome) was one of a small number of specially built monitors that provide exceptional independence between adjacent pixels and high-intensity resolution. This was further verified by demonstrating that look-up table calibrations that incorporate the specific bands of spatial frequencies (corresponding to the classes of experimental stimuli) all yielded the same look-up table values.

4. In regard to possible artifacts, given that the apparatus is producing stimuli correctly, suppose that there was a compressive nonlinearity in the visual system prior to motion detection (see, e.g., Lu & Sperling, 1996a). Might such a nonlinearity distort the stimuli, so that there would be a first-order component in supposedly pure second-order stimuli?

First, a pointwise nonlinearity would not affect binary stimuli, such as the flicker stimuli in this study or the texture contrast stimuli of Nishida (1993). Binary stimuli remain binary stimuli before and after a pointwise nonlinearity. Experimentally, binary stimuli behave quite like the supposedly vulnerable stimuli. All the conclusions of the present study are supported by observations based entirely on binary stimuli.

Second, if a nonlinear compressive nonlinearity produced artifactual first-order components, they would be in the same direction as the presumed second-order component—that is, in the reversed-phi direction. Thus, an artifactually produced first-order component would not contribute to perceived motion opposite to second-order reversed phi—that is, to the third-order motion direction.

Third, there are objective methods of titrating motion stimuli, to measure the amounts of visually produced distortion products. These methods are described elsewhere (Lu & Sperling, 1999). Suffice it to say that, for the second-order reversed-phi stimuli in this study, no significant distortion-produced first-order components were found, although they would easily have been detected if they were present.

(Manuscript received January 5, 1996;
revision accepted for publication June 21, 1998.)